Long noncoding RNA NEAT1 promotes the growth of gastric cancer cells by regulating miR-497-5p/PIK3R1 axis

T.-F. XIA, J. CHEN, K. WU, J. ZHANG, Q. YAN

Department of Gastric Surgery, The Affiliated Huaian No. 1 People's Hospital of Nanjing Medical University, Huai'an City, Jiangsu Province, P.R. China

Abstract. – OBJECTIVE: To investigate the molecular mechanisms of long noncoding RNA (IncRNA) nuclear paraspeckle assembly transcript 1 (NEAT1) in gastric cancer (GC) development progress.

MATERIALS AND METHODS: Relative mR-NA and protein expression levels were quantified by quantitative Reverse Transcription-PCR (qRT-PCR) or Western blot analysis. Cell proliferation and cell apoptosis were measured by MTT (3-(4,5-dimethylthi-azol-2-yl)-2,5-diphenyl tetrazolium bromide) assay and flow cytometry, respectively. Binding sites of miR-497-5p on NEAT1 or phosphoinositide-3-kinase regulatory subunit 1 (PIK3R1) were determined by RNA pull-down assay or dual-luciferase reporter assay. Finally, the tumorigenic role of NEAT1 in GC was assessed using a xenograft model on nude mice.

RESULTS: NEAT1 was upregulated in GC tissues, promoted proliferation, and inhibited apoptosis of GC cells. NEAT1 could directly bind to and negatively regulate miR-497-5p expression. PIK3R1 was then identified as a downstream target of miR-497-5P. In GC cell models, PIK3R1 was found to be directly negatively regulated by miR-497-5p and indirectly positively regulated by NEAT1. Finally, NEAT1 knockdown inhibited tumor growth, increased miR-497-5p expression, and decreased PIK3R1 expression in xenograft model mice compared with the negative control.

CONCLUSIONS: Functioned as an oncogene, NEAT1 promoted cell growth in GC by regulating miR-497-5p/PIK3R1 axis. These results provided valuable insights into the underlying regulation signaling in gastric cancer development, shedding light on NEAT1 a promising therapeutic target from bench to clinic.

Key Words:

NEAT1, MiR-497-5p, PIK3R1, Gastric cancer

Introduction

Gastric cancer (GC) has been considered as one of the most common causes of cancer-related deaths and its pathogenic incidence continues to increase worldwide¹. In China, the incidence and fatality rate of GC are relatively high, only second to lung cancers². Although novel biomarkers for early GC diagnose and multimodal therapy strategies have been developed, the long-term survival rate remains poor³. In 2017, 10,960 patients among the 28,000 newly diagnosed cases are in the possibility of death in the United States⁴. Therefore, it is urgent to investigate the pathogenic mechanisms underlying GC disease progression, as well as to develop new therapeutic strategies and targets.

Long noncoding RNA (lncRNA) are non-coding RNAs of length above 200 nucleotides without a significant open reading frame (ORF)5. LncRNA can directly target and regulate DNA, RNA, and protein targets, by competing with endogenous RNA networks6. Thus, lncRNAs participate in the various cellular and physiological processes by regulating chromatin modification, transcription, and post-transcriptional processing⁷. Nuclear paraspeckle assembly transcript 1 (NEAT1) is a lncRNA and its expression could be induced under various types of stress, such as viral infection⁸, systemic lupus erythematosus⁹, and tumor protein P53 (P53)10-12. Previously Fu JW et al¹³ have shown that NEAT1 expression in GC was corrected with clinical stages, histological types, lymph node metastasis, and distant metastasis by promoting cell migration and invasion. NEAT1 knockdown in GC adriamycin-resistant SGC7901/ADR cells could suppress the malignant biological behaviors and chemotherapy resistance¹⁴. However, the regulating signaling of NEAT1 in GC progression remained unclear.

Chai et al¹⁵ have revealed miR-497-5p might function as an anti-oncogene. The down-regulation of miR-497-5p has been reported in thyroid cancer¹⁶, prostate cancer¹⁷, pancreatic cancer¹⁸, ovarian cancer¹⁹, non-small cell lung cancer²⁰, breast cancer²¹, and colorectal cancer²². Notably, miR-497-5p was proved to promote tumorigenesis in these cancers. In this study, we investigated the role of NEAT1 in GC and further explored the underlying regulating signaling. Our results showed that NEAT1 expression was especially upregulated in GC tissues. NEAT1 promoted proliferation and inhibited apoptosis in GC cells by regulating miR-497-5p/PIK3R1 (phosphoinositide-3-kinase regulatory subunit 1, PIK3R1) axis, suggesting NEAT1 might function as an oncogene and could be considered as a potential diagnostic agent in GC.

Materials and Methods

Tissue Collection

This research was approved by the Animal Ethics Committee of Nanjing Medical University and the informed consent was obtained from all patients diagnosed with GC. GC tissues and adjacent normal tissues were obtained from patients by surgery and immediately frozen in liquid nitrogen at the affiliated Huai'an No.1 People's Hospital of Nanjing Medical University.

Cell Culture

GC cell lines SGC-7901 (BNCC100114), HGC-27 (BNCC338546) were purchased from BeNa Culture Collection Co. Ltd. (Beijing, China). Cells were cultured in Roswell Park Memorial Institute-1640 (RPMI-1640; GIBCO; Thermo Fisher Scientific, Waltham, MA, USA) supplemented with 10% fetal bovine serum (FBS; GIB-CO, Thermo Fisher Scientific, Waltham, MA, USA) and maintained at 37°C in humidified cell incubator (Thermo Fisher Scientific, Waltham, MA, USA) with 5% CO₂.

Quantitative Reverse Transcription-PCR (qRT-PCR)

Total RNAs were isolated from tissues or cells using TRIzol reagent (Invitrogen, Carlsbad, CA, USA) according to the manufacturer's instructions. For NEAT1 analysis, RNAs were reverse transcribed into cDNA with PrimeScript™ RT reagent Kit with gDNA Eraser kit (Takara Biomedical Technology Co., Ltd., Beijing, China)

according to manufacturer's instructions. Then, qRT-PCR was performed using TB GreenTM Premix Ex TagTM II (Takara Biomedical Technology Co., Ltd., Beijing, China) on an ABI PRISM® 7300 real-time PCR system (Applied Biosystems, Foster City, CA, USA) with the primers listed as follows (Table I). For miR-497-5p, RNAs were reverse transcribed into cDNA with miDETECT A TrackTM miRNA qRT-PCR Starter Kit (Guangzhou RiboBio Co., Ltd., Guangzhou, Guangdong, China). Primers used in this study were listed in Table I. Glyceraldehyde-3-phosphate dehydrogenase (GAPDH) and U6 small nuclear 6 (U6) were considered as endogenous controls. Relative expression levels in tissues were calculated using the $2^{-\Delta Ct}$ method.

Western Blotting

Western blot was performed as previously described²³. Briefly, total proteins were extracted from tissues or cells using radioimmunoprecipitation assay (RIPA) buffer (9806; Cell signaling technology, Boston, MA, USA) supplemented with protease inhibitor cocktail (5871; Cell signaling technology, Boston, MA, USA). The concentrations of the extracted proteins were determined using the bicinchoninic acid (BCA) protein assay kit (7780; Cell signaling technology, Boston, MA, USA). 20 µg samples/lane were run on a 10% sodium dodecyl sulfate polyacrylamide gel electrophoresis (SDS-PAGE) and transferred to polyvinylidene difluoride (PVDF) membranes immediately after separation. PVDF membranes were then incubated in 5% (wt/ vol) skimmed milk in Tris Buffered Saline and Tween-20 (TBST) for 120 min at room temperature followed by three 10 min washes in TBST. The PVDF membranes were then incubated with anti-PIK3R1 (1:1000 dilutions, 60225-1-Ig, Proteintech, Wuhan Sanying, Wuhan, Hubei, China), anti-p21 (1:1000 dilutions, 60214-1-Ig, Proteintech, Wuhan Sanying, Wuhan, Hubei, China), anti-cyclin D1 (1:1000 dilutions, 60186-1-Ig, Proteintech, Wuhan Sanying, Wuhan, Hubei, China), anti-Bcl-2 (1:1000 dilu-

Table I. Primers.

Primers	Sequences (5' to 3')		
NEAT1-F	GGGCCATCAGCTTTGAATAA		
NEAT1-R	CTTGAAGCAAGGTTCCAAGC		
miR-497-5p-F	CAGCAGCACACTGTGGTTTGT		
miR-497-5p-R	Provided in the kit		

tions, 60178-1-Ig, Proteintech, Wuhan Sanying, Wuhan, Hubei, China), anti-Bax (1:1000 dilutions, 60267-1-Ig, Proteintech, Wuhan Sanying, Wuhan, Hubei, China), anti-cleaved caspase-3 (1:1000 dilutions, 9661, Cell signaling technology, Boston, MA, USA) and anti-GADPH (1:5000 dilutions, 60004-1-Ig, Proteintech, Wuhan Sanying, Wuhan, Hubei, China) at 4°C overnight. After washing with TBST three times for 10 min each, the membranes were then incubated with appropriate secondary antibody conjugated to horseradish peroxidase (HRP, 1:10000 dilutions). The proteins were visualized using PierceTM ECL Western Blotting Substrate reagent (Thermo Fisher Scientific, Waltham, MA, USA). Semi-quantitative analysis of specific immunolabelling bands was performed using ImageJ (version 1.8.0 112, Bethesda, National Institutes of Health, MD, USA). GAPDH was considered as an internal normalizer.

Luciferase Reporter Assays

Wild type (WT) and mutant 3'untranslated regions (3'UTRs) of PIK3R or NEAT1 were amplified or synthesized, and then inserted into pmiR-GLO vector (E1330, Promega Biotech Co., Beijing, China). For reporter assays, HEK293T cells were co-transfected with reporter plasmids and miR-497-5p mimics using lipofectamine3000 (L3000015, Invitrogen, Thermo Fisher Scientific, Waltham, MA, USA). Firefly and *Renilla* luciferase activities were measured using the dual-luciferase reporter assay system (E1910, Promega Biotech Co., Beijing, China) according to the manufacturer's instructions.

MTT Assay

 110^3 cells were seeded in 96-well plates, 10 μL MTT reagent (Invitrogen, Thermo Fisher Scientific, Waltham, MA, USA) was added to each well and cultured for another 4 h. Then, the medium was discarded and dimethyl sulfoxide (DMSO; Sangon Biotech Co., Ltd., Shanghai, China) was added into each well. After 10 min shaking, OD_{490} was measured using a microplate reader (Thermo Fisher Scientific, Waltham, MA, USA).

Flow Cytometry

Apoptosis was analyzed with Annexin V, FITC Apoptosis Detection Kit (Dojindo Laboratories, Kumamoto, Japan) according to the manufacturer's instructions. In brief, cells were collected, washed, and re-suspended at 110⁶ cells/mL in

1Annexin V Binding Solution. 100 μ L of the suspension was incubated with 5 μ L FITC-Annexin V and propidium iodide (PI) for 15 min in the dark. Then, 400 μ L Annexin V Binding Solution was added and analyzed with FACSCalibur Flow Cytometer (BD Biosciences, Franklin Lakes, NJ, USA).

SGC-7901 Xenograft Model

BALB/c nude mice (male, 4-6-weeks old and 16-20 g) were purchased from the animal experiment center of Nanjing Medical University (Nanjing, Jiangsu, China). All animal experiments were carried out in accordance with the Guide for the Care and Use of Nanjing Medical University. To establish GC xenograft model, 210^6 cells in $200~\mu L$ phosphate-buffered saline (PBS) were inoculated subcutaneously into the flanks of nude mice. The tumor size was monitored by measuring the length (L) and width (W) s every 6 days, and the volumes were calculated as follows: $(LW^2)/2^{24}$.

Mice were sacrificed on day 36 to remove the tumors. Next, the weight of tumors was measured, apoptosis of tumors was detected by TdT-mediated dUTP nick end labeling (TUNEL) assay (C10617; Thermo Fisher Scientific, Waltham, MA, USA), immunohistochemically detection of marker of proliferation Ki-67 (Ki67) was performed and total RNAs and proteins were isolated to measure levels of miR-497-5p and PIK3R1.

Immunohistochemistry

Immunohistochemistry was performed as previously described. In brief, the removed tumors were cut and embedded in paraffin. Then, serial sections (5 µm) were cut and deparaffinized in xylene twice for 10 min each, rehydrated through graded alcohols (100%, 95%, 80% and 60%) for 5 min each, incubated for antigen retrieval in Retrieval Solution (P0086, Beyotime Co., Ltd., Shanghai, China). After incubation with 3% hydrogen peroxide and blocked with 3% bovine serum albumin (BSA), slides were incubated with the ki67 primary antibody (ab15580, Abcam, Cambridge, UK) at 4°C overnight. After washing, slides were incubated with biotinylated anti-rabbit IgG for 45 min (1:200, ab7096, Abcam, Cambridge, UK), followed by ABC complex (A0303, Beyotime Co., Ltd., Shanghai, China). The slides were visualized using diaminobenzidine (DAB; P0203, Beyotime Co., Ltd., Shanghai, China) and counterstained with HE.

Statistical Analysis

All experiments were repeated at least 3 times and results are presented as the means \pm standard error mean (SEM). Statistical analysis was analyzed through SPSS 20.0 software (IBM SPSS, Armonk, NY, USA). To detect significant differences, Student's *t*-test was performed for two groups and Tukey's multiple comparisons test or Dunnett's test after ANOVA test were performed for three or more groups. p<0.05 was considered statistically significant.

Results

Level and Role of NEAT1 in GC Tissues and Cell Models

To explore the role of NEAT1 in GC, NEAT1 expression levels was first quantified in GC tissues. QRT-PCR results showed NEAT1 expression was significantly upregulated in GC tissues compared with adjacent normal tissues (Figure 1 A). Our detailed analysis found the elevated NEAT1 level was significantly associated with the clinic stages of GC and lymphatic metastasis. Meanwhile, NEAT1 expression level was not significantly associated with tumor depth or distant metastasis (Table II), indicating NEAT1 upregulating might be associated with GC progresses.

Subsequently, NEAT1 was knocked down by siRNAs (pLO-#1 NEAT1 and pLO-#2 NEAT1) in SGC-7901 and HGC-27 GC cells, whose transfection efficiency were verified by qRT-PCR. NEAT1 expression was remarkably decreased by siRNA in both cell lines as compared to that in control (NC, pLO-siRNA; Figure 1 B). Then, the cell proliferation and apoptosis were measured by MTT assay and flow cytometry, respectively, showing NEAT1 knockdown significantly inhibited cell growth and promoted cell apoptosis in SGC-7901 and HGC-27 cells (Figure 1 C and D). We also measured the expression levels of the key proteins in the regulation of cell cycle and apoptosis. Cyclin-dependent kinase inhibitor 1A (CDK-N1A, p21) is a cyclin-dependent kinase inhibitor and cyclin D1 is required for progression through the G1 phase of the cell cycle. In SGC-7901 and HGC-27 cells, NEAT1 knockdown elevated protein expression of CDKN1A and decreased cyclin D1 protein expression. BCL2 apoptosis regulator (Bcl-2) level was decreased. In contrast, pro-apoptotic BCL2 Associated X, Apoptosis Regulator (Bax), and cleaved caspase-3 levels were increased (Figure 1 E). Together, our results

suggested NEAT1 was aberrantly expressed as a tumor facilitator in GC.

Effects of MiR-497-5p on GC Cell Models

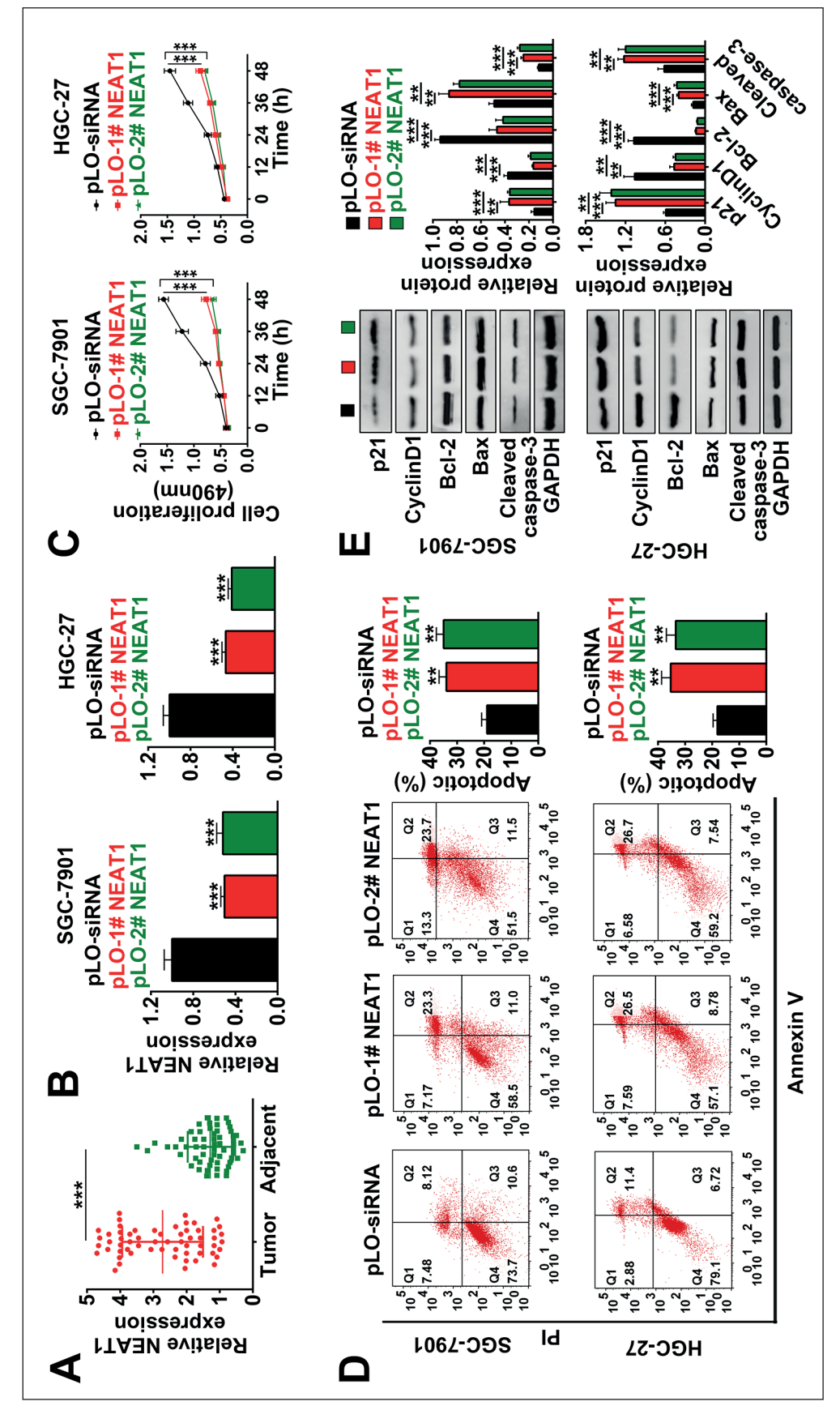
The miR-497-5p level was significantly decreased in GC tissues compared with adjacent normal tissues (Figure 2 A). The chemosynthetic miR-497-5p mimics was employed and transfected into SGC-7901 and HGC-27 cells, whose transfection efficiency was verified (Figure 2 B). MTT assay and flow cytometry illustrated miR-497-5p overexpression inhibited proliferation and promoted apoptosis in SGC-7901 and HGC-27 cells compared to scramble control (NC, miR mimics; Figure 2 C and D). Moreover, miR-497-5p overexpression dramatically enhanced expression levels of CDKN1A, Bax and cleaved caspase-3, as well as decreased levels of cyclin D1 and Bcl-2 (Figure 2 E). Taken together, our data demonstrated miR-497-5p upregulation inhibited proliferation and promoted apoptosis in GC cells.

Relationship Between NEAT1 and MiR-497-5p

The correlations between NEAT1 and miR-497-5p expression in GC tissues were determined by qRT-PCR, suggesting miR-497-5p expression was negatively correlated with NEAT1 level (Figure 3 A). The binding sites of miR-497-5p on NEAT1 were predicted through miRDB (http:// www.mirdb.org/, Figure 3 B). Therefore, we speculated that NEAT1 might negatively regulate expression of miR-497-5p by directly binding to it. To verify our hypothesis, NEAT1 overexpression plasmid was constructed and transfected into SGC-7901 and HGC-27 cells (Figure 3 C). RNA pulldown assay showed miR-497-5p expression was highly enriched by overexpression of NEAT1 (Figure 3 D). Besides, NEAT1 overexpression significantly decreased miR-497-5p level and NEAT1 knockdown could enhance miR-497-5p expression (Figure 3 E). Collectively, these results suggested NEAT1 negatively regulated miR-497-5p expression level as sponges.

PIK3R1 Was a Target of MiR-497-5p

PIK3R1 was predicted to be one of the potential targets of miR-497-5p using TargetScan (http://www.targetscan.org/vert_71/). Therefore, we constructed dual-luciferase reporter plasmids containing WT or mutants of PIK3R1 3'UTR (Figure 4 A). Plasmids containing PIK3R1 3'UTR were co-transfected into 293T cells with



tissues by qRT-PCR. B, Expression of NEAT1 was determined in cells transfected with siRNAs of NEAT1 by qRT-PCR. PLO-siRNA were used as control. C, Cell growth was determined by MTT assay. D, Cell apoptosis was measured by Annexin-V/PI apoptosis detection kit. E, Representative images of Western blot were shown (left). The blots were Figure 1. NEAT1 knockdown inhibited proliferation and promoted apoptosis in GC cells. A, Expression levels of NEAT1 were determined in GC tissues and adjacent normal semi-quantitative analyzed through Image J and normalized to GAPDH (right). **: p<0.01; **** p<0.001

Table II. Correlation between NEAT	1 expression in gastric cance	r specimens and clinicopathological features.

Characteristics	No.	High expression (%)	Low expression (%)	Р
Gender				
Female	26	10 (38.5)	16 (61.5)	0.505
Male	34	16 (47.1)	18 (52.9)	
Age (years)		` /	, ,	
< 50	23	9 (39.1)	14 (60.9)	0.604
≥ 50	37	17 (45.9)	20 (54.1)	
Tumor		,	,	
< 3 cm	32	18 (56.3)	14 (43.7)	0.031
≥ 3 cm	28	8 (28.6)	20 (71.4)	
Clinical stage		, ,	,	
I-II	28	3 (10.7)	25 (89.3)	< 0.001
III-IV	32	23 (71.9)	9 (28.1)	
Tumor depth		,	,	
T1-T2 1	36	15 (41.7)	21 (58.3)	0.750
T3-T4	24	11 (45.8)	13 (54.2)	
Lymph node metastasis		()	- ()	
N0-N1	32	6 (18.8)	26 (81.2)	< 0.001
N2-N3	28	20 (71.4)	8 (28.6)	
Distant metastasis		. (, -, ,)	- (====)	
M0	24	6 (25.0)	18 (75.0)	0.019
M1	36	20 (55.6)	16 (44.4)	

miR-497-5p or NC (miR mimics). Then, the relative luciferase activities were measured. Our results showed mutations on the 3'UTR of PIK3R1 abolished the suppressive ability of miR-497-5p compared with wild type (Figure 4 B left). We also co-transfected luciferase reporter plasmids with NEAT1 overexpression plasmids or NC, further confirming that decrease of miR-497-5p by NEAT1 overexpression could enhance the relative luciferase activities under the condition of WT 3'UTR of PIK3R1 (Figure 4 B right). Furthermore, cells expressing miR-497-5p possessed remarkably decreased PIK3R1 protein level, and cells expressing NEAT1 showed the contrary results (Figure 4 C-D). PIK3R1 was a target of miR-497-5p and NEAT1 could regulate PIK3R1 expression through regulating miR-497-5p.

Effects of NEAT1/MiR-497-5p/PIK3R1 axis In Vitro

To determine whether NEAT1 regulated cell proliferation and cell apoptosis through miR-497-5p/PIK3R1 *in vitro*, we first determined the protein levels of PIK3R1 in cells expressing NEAT1 combined with miR-497-5p mimics or the corresponding controls respectively. Our data showed co-expression of miR-497-5p mimics and NEAT1 abolished NEAT1-induced upregulation of PIK3R1 (Figure 5 A), reversed the promotion effect of NEAT1 on cell proliferation (Figure 5 B), and alleviated the inhibitory effect of NEAT1

on apoptosis (Figure 5 C). Moreover, we found co-expression of miR-497-5p mimics and NEAT1 also reversed expression levels of CDKN1A, cyclin D1, Bcl2, Bax, and cleaved caspase-3 induced by NEAT1 (Figure 5 D), illustrating NEAT1 regulated GC cell proliferation and cell apoptosis through miR-497-5p/PIK3R1 axis *in vitro*.

Effects of NEAT1/MiR-497-5p/PIK3R1 axis In Vivo

We established GC xenograft model using BALB/c nude mice. Tumors expressing siNEAT1 (siNEAT1 group) were smaller than those expressing NC (Vector, NC group; Figure 6 A). Immuno-histochemical results of Ki67 showed that Ki67 expression in siNEAT1 group was much less than that in NC group (Figure 6 B). Apoptosis in siNEAT1 group was promoted than that in the NC group detected by TUNEL assay (Figure 6 C). The miR-497-5p level was increased upon siNEAT1 treatment (Figure 6 D), and PIK3R1 protein level was decreased (Figure 6 E). Our *in vivo* results indicated NEAT1 knockdown could inhibit tumor growth by upregulating miR-497-5p, which in turn decreasing PIK3R1 expression.

Discussion

Due to the development of lncRNA microarray and data mining technology, many lncRNAs

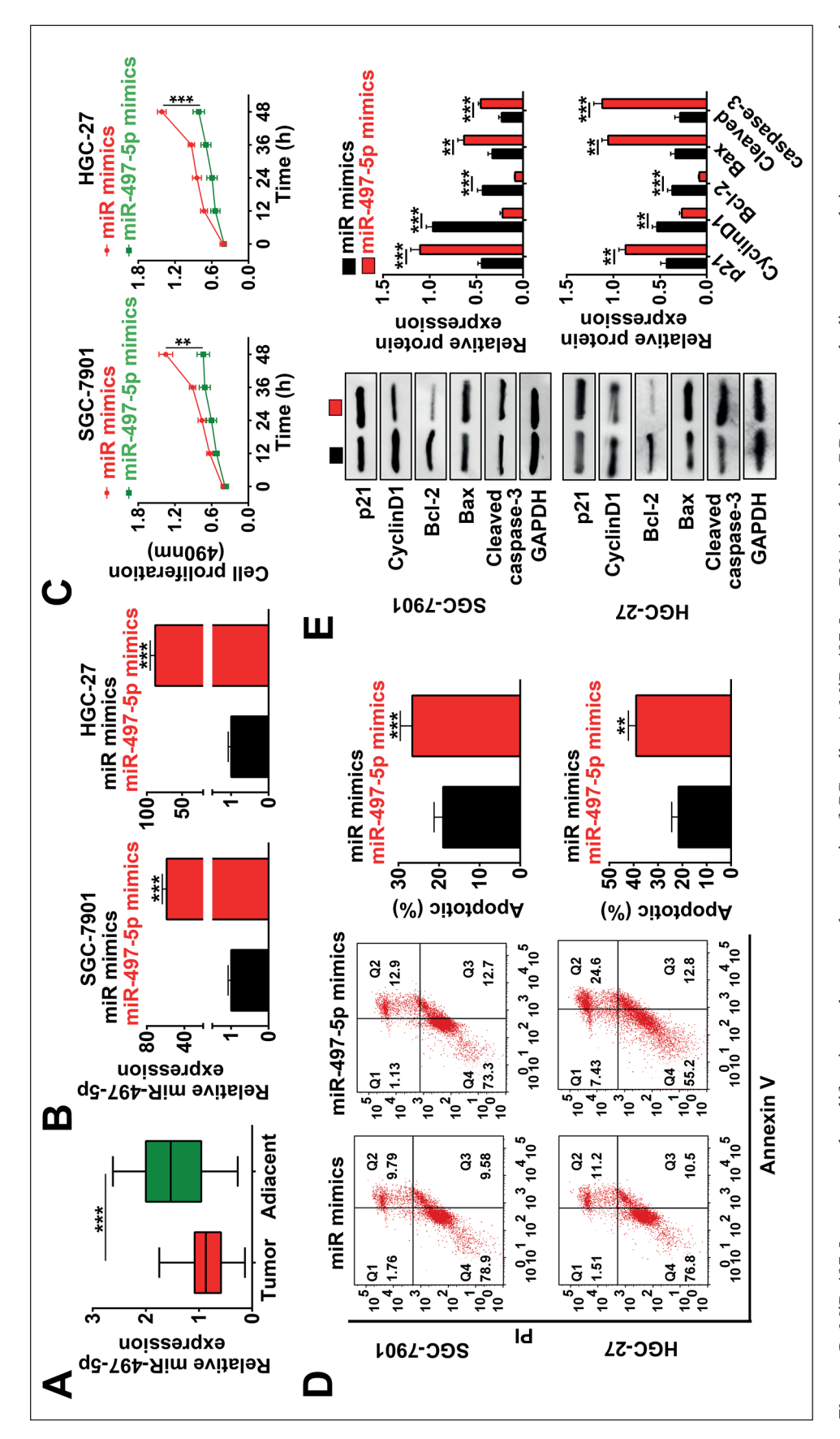


Figure 2. MiR-497-5p suppressed proliferation and promoted apoptosis of GC cells. *A*, MiR-497-5p mRNA levels in GC tissues and adjacent normal tissues were measured by qRT-PCR. *B*, MiR-497-5p expression levels were determined in the cells transfected with miR-497-5p mimics. miR-mimics was used as control (NC). *C*, Cell growth was measured by Annexin-V/PI apoptosis detection kit. *E*, Representative images of Western blot were shown (left). The blots were semi-quantitative analyzed through ImageJ and normalized to GAPDH (right). **: p < 0.001; ***: p < 0.001.

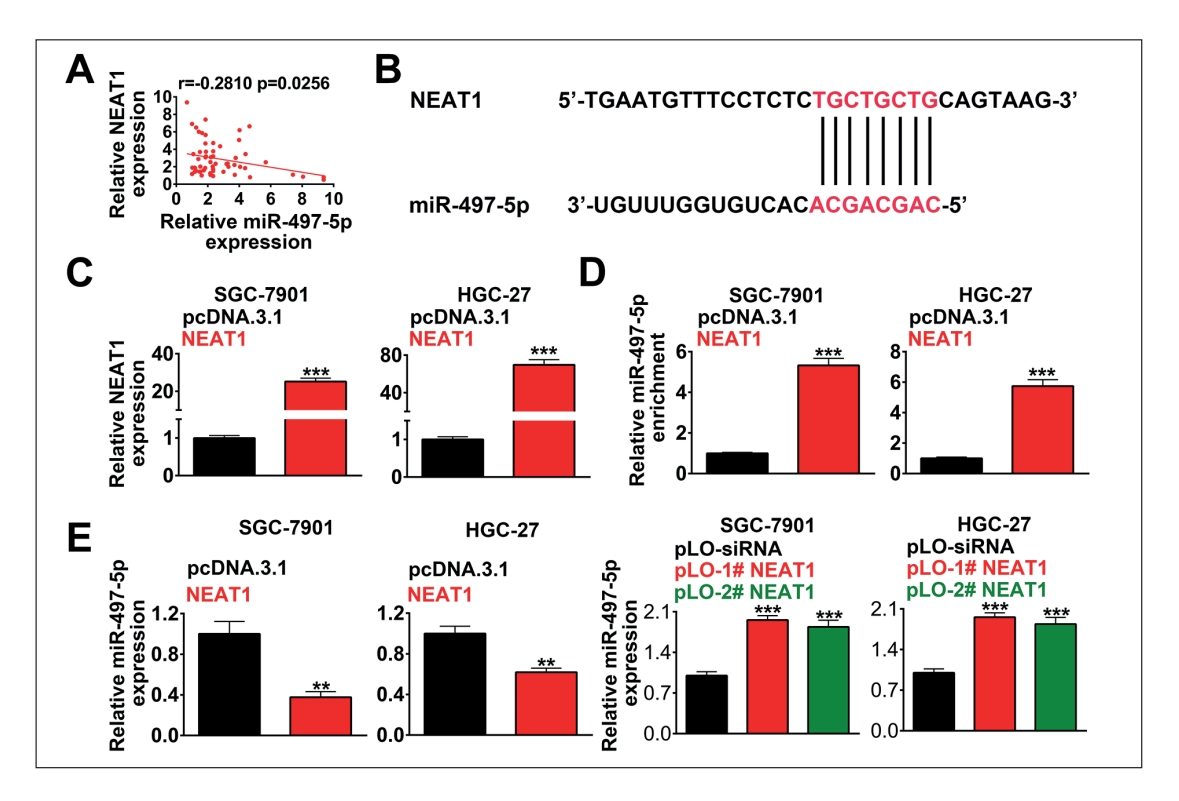


Figure 3. NEAT1 negatively regulated expression of miR-497-5p. *A*, Correlation analysis of expression of NEAT1 and miR-497-5p in GC tissues. *B*, Predicted miR-497-5p binding sites on NEAT1. *C*, Expression levels of NEAT1 in the cells were determined by qRT-PCR. pcDNA3.1: empty vector used as control; NEAT1: NEAT1 in pcDNA3.1 vector. *D*, Overexpression of NEAT1 enriched miR-497-5p efficiently in GC cells. *E*, Expression of miR-497-5p were determined by RT-qPCR. **: *p*<0.01; ***: *p*<0.001.

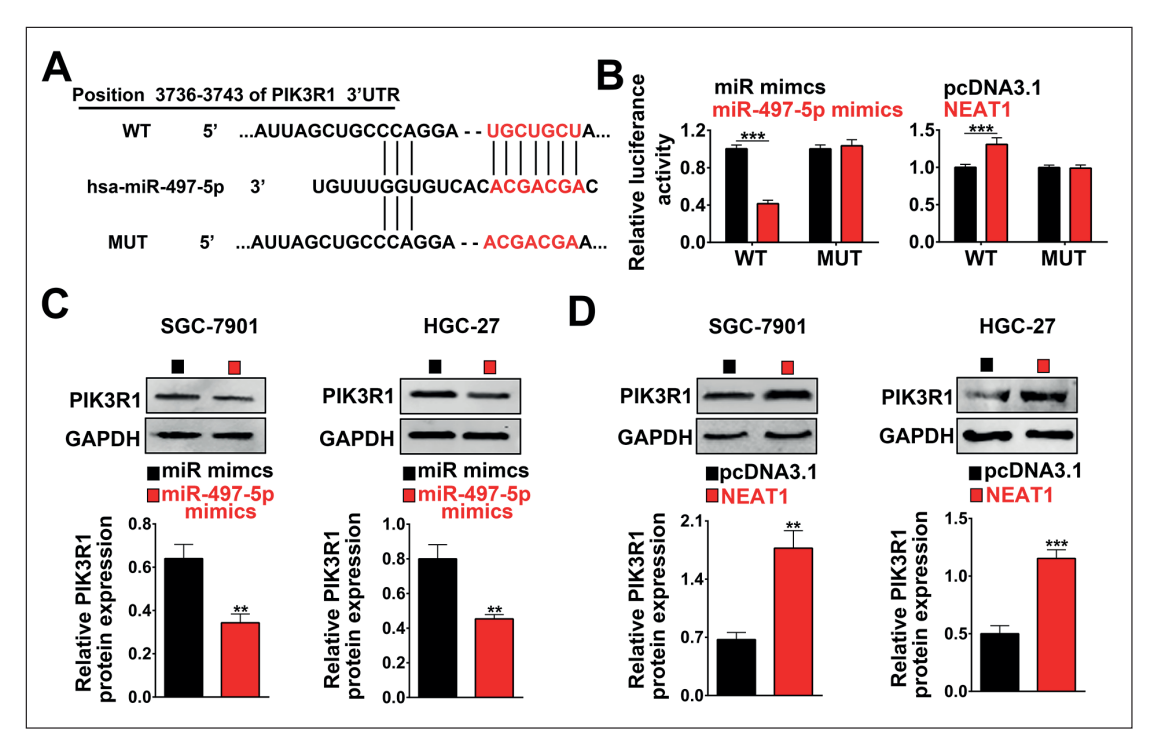


Figure 4. PIK3R1 was a target of miR-497-5p. A, Diagram of binding sites of miR-497-5p on 3'UTR of PIK3R1. B, Relative luciferase activities of cell lysis were measured. C, D, Representative images of Western blot were shown (top). The blots were semi-quantitative analyzed through ImageJ and normalized to GAPDH (bottom). **: p < 0.01; ***: p < 0.001.

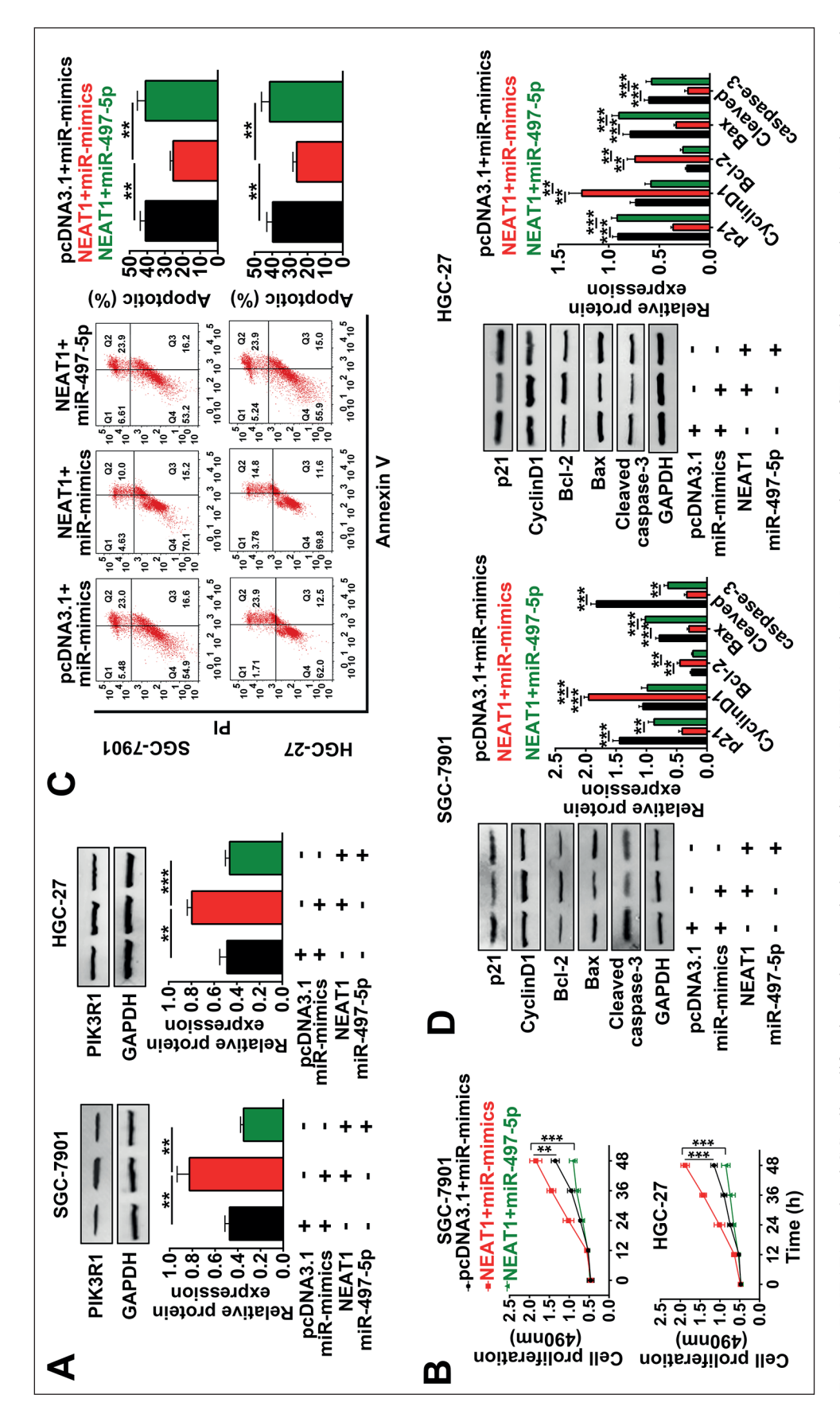


Figure 5. NEAT1 regulated GC cell proliferation and apoptosis through miR-497-5p/PIK3R1 axis. A, Representative images of Western blot were shown (top). Blots were semiquantitative analyzed through ImageJ and normalized to GAPDH (bottom). B, Cell proliferation was determined by MTT assay. C, Cell apoptosis was measured by Annexin-V/PI apoptosis detection kit. D, Representative images of Western blot were shown and the blots were semi-quantitative analyzed through ImageJ and normalized to GAPDH. **: p<0.01; ***: p<0.001

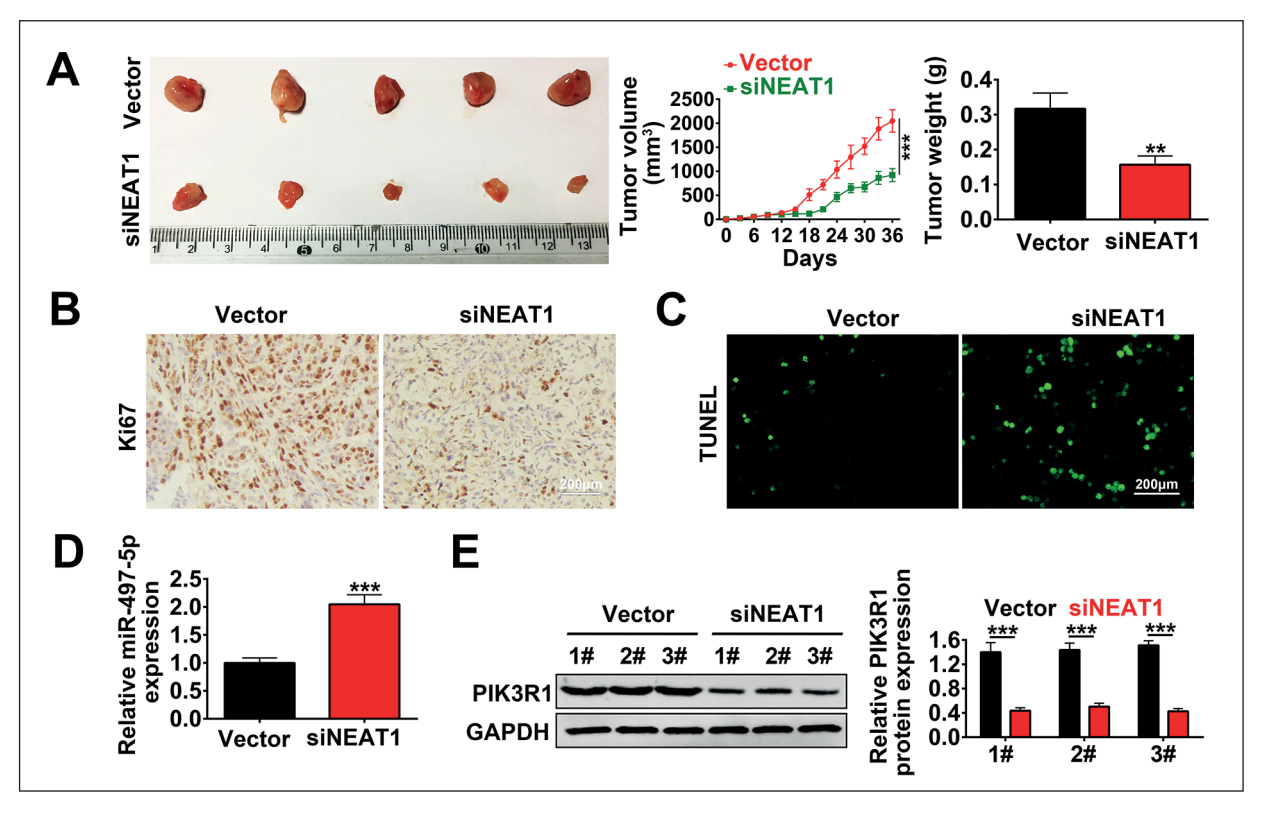


Figure 6. NEAT1 knock-own inhibited tumor growth *in vivo. A*, Representative pictures of excised tumors (left), tumor growth curves (middle) and weight (right) of the excised tumors were shown. siNEAT1: NEAT1 knockdown group; Vector: control group (NC). **B**, Representative pictures of expression of Ki67 detected with immunohistochemical staining were shown. **C**, Representative pictures of TUNEL assay were shown. **D**, Expression levels of miR-497-5p in tumors were measured by qRT-PCR. **E**, Representative images of Western blot detecting PIK3R1 in tumors were shown (left). The blots were semi-quantitative analyzed through ImageJ and normalized to GAPDH (right). **: p<0.01; ***: p<0.001.

were found differentially expressed in GC tissues. which have been considered as novel diagnostic and prognosis biomarkers in tumorigenesis of GC^{25,26}. In this study, we discovered NEAT1 was aberrantly upregulated in GC tissues compared with adjacent normal tissues. Our GC cell model further confirmed NEAT1 promoted cell proliferation and inhibited cell apoptosis in vitro and in vivo. Wang et al27 draw a similar conclusion i.e., that NEAT1 was upregulated in GC, which promoted cell viability and migration by controlling the expression of miR-17. Researches²⁸⁻³⁵ also reported NEAT1 was aberrantly expressed in endometrial endometrioid adenocarcinoma, cervical carcinoma, multiple myeloma, hepatocellular carcinoma, clear cell renal cell carcinoma, colorectal cancer, and glioma. These results suggested that NEAT1 functioned as an oncogene in tumorigenesis.

Previous studies^{36,37} revealed miR-497-5p level was decreased in various types of cancers. A decreased miR-497-5p expression could promote

cell proliferation, migration, invasion, and inhibit apoptosis. Consistently, we discovered similar miR-497-5p-mediated cellular events in GC. Of note, we confirmed that a decreased miR-497-5p level was negatively correlated with NEAT1 expression in GC tissues. The binding sites between NEAT1 and miR-497-5p were validated by RNA pull-down assay, and the miR-497-5p level was negatively regulated by NEAT1 in GC cells.

Our further work identified PIK3R1 as a target of miR-497-5p in GC cells. NEAT1 overexpression in GC cells upregulated PIK3R1 level by suppressing miR-497-5p expression. Based on these foundations, we performed "rescue" experiments to verify our hypothesis. Co-expression of miR-497-5p and NEAT1 significantly abolished the NEAT1 overexpression-altered PIK3R1 level, cell proliferation, and apoptosis *in vitro* experiment. The *in vivo* experiment in xenograft model exhibited NEAT1 knockdown, inhibited the tumor growth, and miR-497-5p was upregulated, and adversely, PIK3R1

was downregulated. Taken together, our results suggested NEAT1 functioned as an oncogene in GC through the miR-497-5p/PIK3R1 axis. In breast cancer, miR-497-5p suppressed angiogenesis or inhibited epithelial-mesenchymal transition (EMT) by targeting *hypoxia-inducible* factor 1 subunit alpha (HIF-1a), or snail family transcriptional repressor 2 (Slug)^{21,38,39}. In cervical cancer and colorectal cancer, miR-475-5p played a tumor-suppressive role by targeting insulin-like growth factor 1 receptor (IGF1R)^{22,40}. In GC, miR-497-5p inhibited cell proliferation and invasion via eukaryotic translation initiation factor 4E (eIF4E)⁴¹, indicating miR-497-5p could regulate cellular function through different targets. However, an in-depth study regarding whether NEAT1 functioned as an oncogene through other targets (such as IGF1R oreIF4E) via miR-497-5p in GC needs to be further investigated.

PIK3R1 encodes the regulatory subunit of class I phosphoinositide 3 kinases (PI3Ks), which could regulate various cellular functions and was involved in tumorigenesis via PI3K/phosphatase and tensin homolog (PTEN)/protein kinase B (AKT) pathway⁴². However, the role of PIK3R1 seems contradictory in different types of cancers. Decreased PIK3R1 level has been reported in prostate cancer, lung cancer, and liver cancers. Liver-specific deletion of PIK3R1 in mice promoted live tumorigenesis through the PI3K/ PTEN/AKT pathway43. Huang et al44 reported PIK3R1 was upregulated in hepatocellular carcinoma and promoted tumor progression. Thus, PIK3R1 might exert dual functions in tumorigenesis. In this study, we discovered PIK3R1 level could be induced by NEAT1 in GC and subsequently promoted GC progression.

Conclusions

We suggested NEAT1 could function as an oncogene in GC by upregulating PIK3R1 expression via decreasing miR-497-5p expression, which provided valuable insights into the underlying regulation signaling in gastric cancer development, shedding lights on NEAT1 as promising therapeutic target from bench to clinic.

Conflict of Interest

The Authors declare that they have no conflict of interests.

References

- CHIVU-ECONOMESCU M, MATEI L, NECULA LG, DRAGU DL, BLEOTU C, DIACONU CC. New therapeutic options opened by the molecular classification of gastric cancer. World J Gastroenterol 2018; 24: 1942-1961.
- 2) SHU Y, ZHANG W, HOU Q, ZHAO L, ZHANG S, ZHOU J, SONG X, ZHANG Y, JIANG D, CHEN X, WANG P, XIA X, LIAO F, YIN D, CHEN X, ZHOU X, ZHANG D, YIN S, YANG K, LIU J, FU L, ZHANG L, WANG Y, ZHANG J, AN Y, CHENG H, ZHENG B, SUN H, ZHAO Y, WANG Y, XIE D, OUYANG L, WANG P, ZHANG W, QIU M, FU X, DAI L, HE G, YANG H, CHENG W, YANG L, LIU B, LI W, DONG B, ZHOU Z, WEI Y, PENG Y, XU H, HU J. Prognostic significance of frequent CLDN18-ARHGAP26/6 fusion in gastric signet-ring cell cancer. Nat Commun 2018; 9: 2447.
- 3) ZHANG J, LIU X, YU G, LIU L, WANG J, CHEN X, BIAN Y, JI Y, ZHOU X, CHEN Y, JI J, XIANG Z, GUO L, FANG J, SUN Y, CAO H, ZHU Z, YU Y. UBE2C is a potential biomarker of intestinal-type gastric cancer with chromosomal instability. Front Pharmacol 2018; 9: 847.
- 4) Wang YL, GE XX, Wang Y, Xu MD, Gong FR, Tao M, Wang WJ, Shou LM, Chen K, Wu MY, Li W. The values of applying classification and counts of white blood cells to the prognostic evaluation of resectable gastric cancers. BMC Gastroenterol 2018; 18: 99.
- Anastasiadou E, Faggioni A, Trivedi P, Slack FJ. The nefarious nexus of noncoding RNAs in cancer. Int J Mol Sci 2018; 19. pii: E2072.
- Dong BS, Shi MJ, Su SB, Zhang H. Insight into long noncoding competing endogenous RNA networks in hepatic fibrosis: the potential implications for mechanism and therapy. Gene 2019; 687: 255-260.
- MARCHESE FP, RAIMONDI I, HUARTE M. The multidimensional mechanisms of long noncoding RNA function. Genome Biol 2017; 18: 206.
- WANG Z, FAN P, ZHAO Y, ZHANG S, LU J, XIE W, JIANG Y, LEI F, XU N, ZHANG Y. NEAT1 modulates herpes simplex virus-1 replication by regulating viral gene transcription. Cel Mol Life Sci 2017; 74: 1117-1131.
- 9) ZHANG F, Wu L, QIAN J, QU B, XIA S, LA T, WU Y, MA J, ZENG J, GUO Q, CUI Y, YANG W, HUANG J, ZHU W, YAO Y, SHEN N, TANG Y. Identification of the long noncoding RNA NEAT1 as a novel inflammatory regulator acting through MAPK pathway in human lupus. J Autoimmun 2016; 75: 96-104.
- IDOGAWA M, OHASHI T, SASAKI Y, NAKASE H, TOKINO T. Long non-coding RNA NEAT1 is a transcriptional target of p53 and modulates p53-induced transactivation and tumor-suppressor function. Int J Cancer 2017; 140: 2785-2791.
- MELLO SS, SINOW C, RAJ N, MAZUR PK, BIEGING RK, BROZ DK, IMAM JFC, VOGEL H, WOOD LD, SAGE J, HI-ROSE T, NAKAGAWA S, RINN J, ATTARDI LD. Neat1 is a p53-inducible lincRNA essential for transformation suppression. Genes Dev 2017; 31: 1095-1108.

- 12) SUN C, LI S, ZHANG F, XI Y, WANG L, BI Y, LI D. Long non-coding RNA NEAT1 promotes non-small cell lung cancer progression through regulation of miR-377-3p-E2F3 pathway. Oncotarget 2016; 7: 51784-51814.
- 13) Fu JW, Kong Y, Sun X. Long noncoding RNA NEAT1 is an unfavorable prognostic factor and regulates migration and invasion in gastric cancer. J Cancer Res Clin Oncol 2016; 142: 1571-1579.
- 14) ZHANG J, ZHAO B, CHEN X, WANG Z, XU H, HUANG B. Silence of long noncoding RNA NEAT1 inhibits malignant biological behaviors and chemotherapy resistance in gastric cancer. Pathol Oncol Res 2018; 24: 109-113.
- 15) Chai L, Kang X, Sun Z, Zeng M, Yu S, Ding Y, Liang J, Li T, Zhao J. MiR-497-5p, miR-195-5p and miR-455-3p function as tumor suppressors by targeting hTERT in melanoma A375 cells. Cancer Manag Res 2018; 10: 989-1003.
- 16) WANG P, MENG X, HUANG Y, LV Z, LIU J, WANG G, MENG W, XUE S, ZHANG Q, ZHANG P, CHEN G. MicroR-NA-497 inhibits thyroid cancer tumor growth and invasion by suppressing BDNF. Oncotarget 2017; 8: 2825-2834.
- 17) Kong XJ, Duan LJ, Qian XQ, Xu D, Liu HL, Zhu YJ, Qi J. Tumor-suppressive microRNA-497 targets IKKbeta to regulate NF-kappaB signaling pathway in human prostate cancer cells. Am J Cancer Res 2015; 5: 1795-1804.
- 18) Xu J, WANG T, CAO Z, HUANG H, LI J, LIU W, LIU S, YOU L, ZHOU L, ZHANG T, ZHAO Y. MiR-497 downregulation contributes to the malignancy of pancreatic cancer and associates with a poor prognosis. Oncotarget 2014; 5: 6983-6993.
- 19) WANG W, REN F, WU Q, JIANG D, LI H, SHI H. MicroRNA-497 suppresses angiogenesis by targeting vascular endothelial growth factor A through the PI3K/AKT and MAPK/ERK pathways in ovarian cancer. Oncol Rep 2014; 32: 2127-2133.
- 20) ZHAO W, WANG Y, AN Z, SHI C, ZHU G, WANG B, LU M, PAN C, CHEN P. Downregulation of miR-497 promotes tumor growth and angiogenesis by targeting HDGF in non-small cell lung cancer. Biochem Bioph Res Commun 2013; 435: 466-471.
- 21) Wei C, Luo Q, Sun X, Li D, Song H, Li X, Song J, Hua K, Fang L. MicroRNA-497 induces cell apoptosis by negatively regulating Bcl-2 protein expression at the posttranscriptional level in human breast cancer. International J Clin Exp Pathol 2015; 8: 7729-7739.
- 22) Guo ST, Jiang CC, Wang GP, Li Y, Wang CY, Guo XY, Yang H, Feng Y, Wang F, Tseng H, Thorne RF, Jin L, Zhang XD. MicroRNA-497 targets insulin-like growth factor 1 receptor and has a tumour suppressive role in human colorectal cancer. Oncogene 2013; 32: 1910-1920.
- 23) Morisaki T, Yashiro M, Kakehashi A, Inagaki A, Kinoshita H, Fukuoka T, Kasashima H, Masuda G, Sakurai K, Kubo N, Muguruma K, Ohira M, Wanibu-

- CHI H, HIRAKAWA K. Comparative proteomics analysis of gastric cancer stem cells. PloS One 2014; 9: e110736.
- 24) Marshall DJ, Harried SS, Murphy JL, Hall CA, Shekhani MS, Pain C, Lyons CA, Chillemi A, Malavasi F, Pearce HL, Thorson JS, Prudent JR. Extracellular antibody drug conjugates exploiting the proximity of two proteins. Mol Ther 2016; 24: 1760-1770.
- 25) Song H, Sun W, Ye G, Ding X, Liu Z, Zhang S, Xia T, Xiao B, Xi Y, Guo J. Long non-coding RNA expression profile in human gastric cancer and its clinical significances. J Transl Med 2013; 11: 225.
- 26) TIAN X, ZHU X, YAN T, YU C, SHEN C, HONG J, CHEN H, FANG J. Differentially expressed IncRNAs in gastric cancer patients: a potential biomarker for gastric cancer prognosis. J Cancer 2017; 8: 2575-2586.
- 27) WANG CL, WANG D, YAN BZ, FU JW, QIN L. Long non-coding RNA NEAT1 promotes viability and migration of gastric cancer cell lines through up-regulation of microRNA-17. Eur Rev Med Pharmacol Sci 2018; 22: 4128-4137.
- 28) Li Z, Wei D, Yang C, Sun H, Lu T, Kuang D. Overexpression of long noncoding RNA, NEAT1 promotes cell proliferation, invasion and migration in endometrial endometrioid adenocarcinoma. Biomed Pharmacother 2016; 84: 244-251.
- 29) Guo HM, Yang SH, Zhao SZ, Li L, Yan MT, Fan MC. LncRNA NEAT1 regulates cervical carcinoma proliferation and invasion by targeting AKT/ PI3K. Eur Rev Med Pharmacol Sci 2018; 22: 4090-4097.
- 30) Xu H, Li J, Zhou ZG. NEAT1 promotes cell proliferation in multiple myeloma by activating Pl3K/ AKT pathway. Eur Rev Med Pharmacol Sci 2018; 22: 6403-6411.
- 31) WANG Z, ZOU Q, SONG M, CHEN J. NEAT1 promotes cell proliferation and invasion in hepatocellular carcinoma by negative regulating miR-613 expression. Biomed Pharmacother 2017; 94: 612-618.
- 32) NING L, LI Z, WEI D, CHEN H, YANG C. LncRNA, NEAT1 is a prognosis biomarker and regulates cancer progression via epithelial-mesenchymal transition in clear cell renal cell carcinoma. Cancer Biomark 2017; 19: 75-83.
- PENG W, WANG Z, FAN H. LncRNA NEAT1 impacts cell proliferation and apoptosis of colorectal cancer via regulation of akt signaling. Pathol Oncolo Res 2017; 23: 651-656.
- 34) YANG X, XIAO Z, Du X, HUANG L, Du G. Silencing of the long non-coding RNA NEAT1 suppresses glioma stem-like properties through modulation of the miR-107/CDK6 pathway. Oncol Rep 2017; 37: 555-562.
- 35) ZHEN L, YUN-HUI L, HONG-YU D, JUN M, YI-LONG Y. Long noncoding RNA NEAT1 promotes glioma pathogenesis by regulating miR-449b-5p/c-Met axis. Tumor Biol 2016; 37: 673-683.

- 36) CHEN Y, KUANG D, ZHAO X, CHEN D, WANG X, YANG Q, WAN J, ZHU Y, WANG Y, ZHANG S, WANG Y, TANG Q, MASUZAWA M, WANG G, DUAN Y. MiR-497-5p inhibits cell proliferation and invasion by targeting KCa3.1 in angiosarcoma. Oncotarget 2016; 7: 58148-58161.
- CHEN X, SHI C, WANG C, LIU W, CHU Y, XIANG Z, HU K, DONG P, HAN X. The role of miR-497-5p in myo-fibroblast differentiation of LR-MSCs and pulmonary fibrogenesis. Sci Rep 2017; 7: 40958.
- Wu Z, CAI X, Huang C, Xu J, Liu A. MiR-497 suppresses angiogenesis in breast carcinoma by targeting HIF-1α. Oncol Rep 2016; 35: 1696-1702
- Wu Z, Li X, Cai X, Huang C, Zheng M. MiR-497 inhibits epithelial mesenchymal transition in breast carcinoma by targeting Slug. Tumor Biol 2016; 37: 7939-7950.
- 40) Luo M, Shen D, Zhou X, Chen X, Wang W. MicroR-NA-497 is a potential prognostic marker in human cervical cancer and functions as a tumor sup-

- pressor by targeting the insulin-like growth factor 1 receptor. Surgery 2013; 153: 836-847.
- 41) Li W, Jin X, Deng X, Zhang G, Zhang B, Ma L. The putative tumor suppressor microRNA-497 modulates gastric cancer cell proliferation and invasion by repressing elF4E. Biochem Bioph Res Co 2014; 449: 235-240.
- 42) HAMIDI A, SONG J, THAKUR N, ITOM S, MARUSSON A, BERGH A, HELDIN CH, LANDSTRÖM M. TGF-beta promotes PI3K-AKT signaling and prostate cancer cell migration through the TRAF6-mediated ubiquitylation of p85α. Sci Signal 2017; 10. pii: eaal4186.
- 43) MARSHALL JDS, WHITECROSS DE, MELLOR P, ANDERSON DH. Impact of p85α alterations in cancer. Biomolecules 2019; 9: 29. pii: E29.
- 44) Huang XP, Hou J, Shen XY, Huang CY, Zhang XH, XIE YA, Luo XL. MicroRNA-486-5p, which is downregulated in hepatocellular carcinoma, suppresses tumor growth by targeting PIK3R1. FEBS J 2015; 282: 579-594.